Journal of the Association of Arab Universities for Basic and Applied Sciences (2016) 21, 17–23

University of Bahrain

Journal of the Association of Arab Universities for Basic and Applied Sciences

www.elsevier.com/locate/jaaubas
www.sciencedirect.com

ORIGINAL ARTICLE

Efficient adsorption of 4-Chloroguiacol from aqueous solution using optimal activated carbon: Equilibrium isotherms and kinetics modeling

Afidah Abdul Rahim [a], **Zaharaddeen N. Garba** [a,b,*]

[a] *School of Chemical Sciences, Universiti Sains Malaysia, 11800 Penang, Malaysia*
[b] *Department of Chemistry, Ahmadu Bello University, P.M.B. 1044, Zaria, Nigeria*

Received 28 July 2015; revised 31 August 2015; accepted 3 September 2015
Available online 29 November 2015

KEYWORDS

Prosopis africana seed hulls;
Activated carbon;
Isotherms and kinetics modeling;
Adsorption;
4-Chloroguiacol

Abstract The optimal activated carbon produced from *Prosopis africana* seed hulls (PASH-AC) was obtained using the impregnation ratio of 3.19, activation temperature of 780 °C and activation time of 63 min with surface area of 1095.56 m^2/g and monolayer adsorption capacity of 498.67 mg/g. The adsorption data were also modeled using five various forms of the linearized Langmuir equations as well as Freundlich and Temkin adsorption isotherms. In comparing the legitimacy of each isotherm model, chi square (χ^2) was incorporated with the correlation coefficient (R^2) to justify the basis for selecting the best adsorption model. Langmuir-2 > Freundlich > Temkin isotherms was the best order that described the equilibrium adsorption data. The results revealed pseudo-second-order to be the most ideal model in describing the kinetics data.

1. Introduction

Recently, one of the most troubling environmental challenges troubling developing countries is water pollution (Galadima et al., 2011). Thousands of these water pollutants are chemical contaminants with many of them of organic origin which include chlorophenols. Guaiacols are among those chemical contaminants with pharmacological properties quite analogous to those of phenol. Chlorinated guaiacols are closely related to chlorophenols.

Adsorption is one of the most useful and effective among the control technologies (El Haddad et al., 2012, 2013; Noreen and Bhatti, 2014; Noreen et al., 2013) for the waste water treatment with the most broadly employed adsorbent being activated carbon due to simplicity in design, lofty adsorption capacity and fast adsorption kinetics (Garba et al., 2014). Activated carbons (AC) are the most sought after adsorbents (Jodeh et al., 2016) due to their versatile surface characteristics, widely utilized for a variety of industrial applications. The conversion of an agricultural waste material into a useful commodity toward the removal of a potential contaminant seems to be an attractive way in economic as well as environmental point of view.

Optimum conditions for AC preparation from PASH have been reported in our earlier studies but no work has been reported to be done on the adsorption application of the

* Corresponding author at: School of Chemical Sciences, Universiti Sains Malaysia, 11800 Penang, Malaysia. Tel.: +60 1126116051, +234 8039443335.
E-mail address: dinigetso2000@gmail.com (Z.N. Garba).
Peer review under responsibility of University of Bahrain.

http://dx.doi.org/10.1016/j.jaubas.2015.09.001

optimal PASH-AC on any type of adsorbate which constitutes the novelty of our work.

This work is therefore aimed at investigating the effect of initial 4CG concentration, adsorption time and pH of the solution on the optimal activated carbon (PASH-AC) using potassium oxalate ($K_2C_2O_4$) as chemical activating agent for the removal of 4-Chloroguiacol (4CG). Kinetic, equilibrium data modeling as well as thermodynamics study of the spent PASH-AC were also investigated. Similar experiments were carried out under the same conditions with commercial activated carbon for comparison.

2. Materials and methods

2.1. Adsorbate (4-Chloroguiacol)

Sigma–Aldrich (M) Sdn Bhd, Malaysia supplied the adsorbate (4CG) used with all the solutions prepared using deionized water. 4CG has a molecular weight of 158.58 g/mol with chemical formula of C_7H_7ClO.

2.2. Preparation of adsorbent (PASH-AC)

Prosopis africana seed hulls (PASH) used as the precursor was collected from Nigeria. The procedure employed in producing the PASH-AC was as reported in our erstwhile work (Garba and Afidah, 2014) where the precursor (PASH) was impregnated with the $K_2C_2O_4$. The optimum preparation conditions applied were as obtained in our previous work (Garba and Afidah, 2014) which produced PASH-AC with reasonable yield and significant 4CG removal.

2.3. Removal of 4CG by batch adsorption

Batch adsorption experiments for the 4CG removal by PASH-AC were conducted as reported in our formerly published work (Garba et al., 2014).

The 4CG percentage removed at equilibrium ($\%R$) was evaluated as:

$$\text{4CG removal } (\%) = \frac{C_o - C_e}{C_o} \times 100 \quad (1)$$

where the initial and equilibrium concentrations are denoted as C_o and C_e (mg/L), respectively.

The adsorbed equilibrium amount of 4CG, q_e (mg/g), was estimated by Eq. (2):

$$q_e = \frac{(C_o - C_e)V}{W} \quad (2)$$

In order to analyze kinetics of the adsorption process, the 4CG concentration was evaluated at interludes of time. The 4CG amount adsorbed at time t, q_t (mg/g) was evaluated using Eq. (3):

$$q_t = \frac{(C_o - C_t)V}{W} \quad (3)$$

The pH of the solution was adjusted with 0.1 M HCl and 0.1 M KOH solutions in order to study the effect of initial pH (2–12) on the 4CG adsorption by PASH-AC and measured using a pH meter (Martini instrument, Mi 150).

Fourier Transform Infrared (FTIR) spectroscopy (FTIR-2000, PerkinElmer) with KBr technique was used in analysing the functional groups on the precursor as well as the PASH-AC surface. The spectra were documented from 4000 to 400 cm^{-1}.

3. Results and discussion

3.1. Characterization of PASH-AC

The spectra of precursor and PASH-AC in Fig. 1 show an increase and/or decrease of peaks. The broad bands between 3500 and 3200 cm^{-1} on the spectra signify the presence of O–H or N–H functional groups, peaks between 3300–3000 cm^{-1} and 3000–2800 cm^{-1} have been allotted to unsaturated as well as saturated C–H respectively, those bands at 1800–1600 cm^{-1}, 1600–1700 cm^{-1} and 1500–1600 cm^{-1} were for C═O, C═C or aromatic rings and C≡N respectively (Shi et al., 2010). The bands between 1500 and 1400 cm^{-1} connote the presence of C–C stretching, additionally, the presence of C–O stretching in carboxyl acids, alcohols, phenols and esters was justified by the bands between 1260 and 1050 cm^{-1}. The weak peak located between 700 and 800 was designated to C–OH (out of plane bending) in phenol. As can be seen from the spectra, numerous functional groups vanished after carbonization and activation processes. This was attributed to thermal degradation effect which resulted in the destruction of some intermolecular bonding.

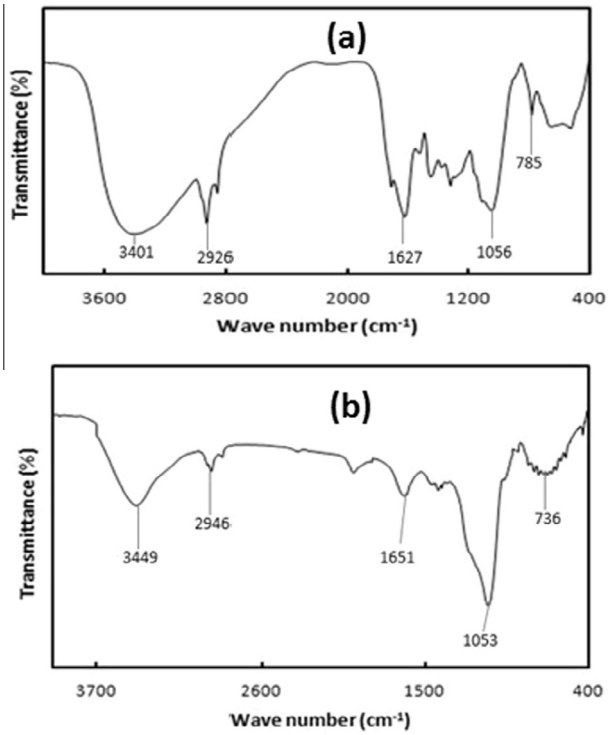

Figure 1 FT-IR spectra for (a) PASH and (b) PASH-AC.

3.2. Influence of adsorption time and 4CG concentrations

The influence of adsorption time on the 4CG removal by PASH-AC for six different adsorbate concentrations at 30 °C is described in Fig. 2. Rapid increase of the 4CG concentrations can be observed from the start, with much slower uptake following until equilibrium was established.

Equilibrium position was attained at shorter time for lower initial concentrations than at higher initial concentrations as can be observed. The difference in equilibrium time attainment was attributed to the faster extinction or disappearance of adsorbate molecules at different initial concentrations (Hameed et al., 2008). The influence of potassium oxalate activating agent for the development of mesoporous and high surface area of PASH-AC with numerous functional groups as seen in characterization results enhanced the faster adsorption process observed.

3.3. Effect of solution pH

Charge on adsorbent surface, functional group detachment on its effective sites, the extent of ionization as well as structural changes of adsorbate molecules can be influenced by solution pH. As shown in Fig. 3, 4CG percentage removal shows a significant decrease with an upsurge in the solution pH from 2 to 12. The percentage removal, as high as 95.81% was achieved at pH 2, which was attributed to its high tendency of hydrogen bond formation with the surface of the PASH-AC due to the withdrawing group effect exerted by the methoxy group (Hamad et al., 2011).

3.4. Adsorption isotherm modeling

Three most popular isotherm models (Temkin, Langmuir as well as Freundlich) were applied to probe the equilibrium data.

Langmuir isotherm is one of the highly popular isotherms for the removal of dyes as well as other organic pollutants by adsorption onto activated carbon. The model is explained by Eq. (4) (Langmuir, 1916):

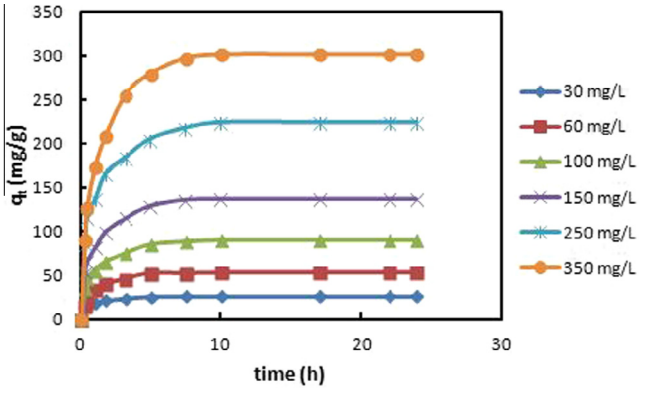

Figure 2 Effect of contact time on 4CG adsorption onto PASH-AC at various initial concentrations.

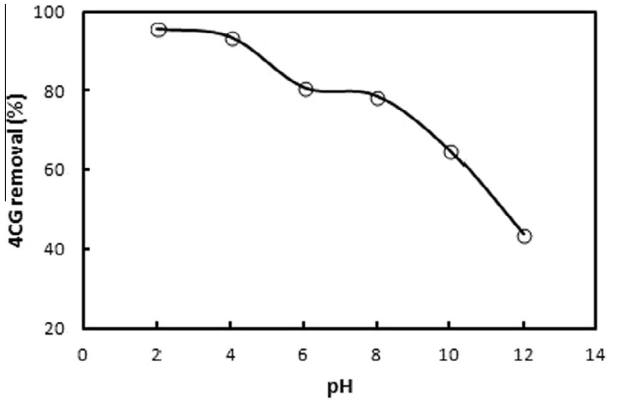

Figure 3 Effect of solution pH on 4CG removal by PASH-AC.

$$q_e = \frac{K_L Q_a^0 C_e}{1 + K_L C_e} \tag{4}$$

The isotherm constants associated with adsorption capacity and rate of adsorption were symbolized as Q_a^0 (mg/g) and K_L (L/mg) respectively. Eq. (4) was expressed in five different linear forms, as tabulated in Table 1, with their major main disparities connected to the distribution of data as well as the parameter determination accuracy (Baccar et al., 2013).

The term describing essential characteristics of the monolayer equation is referred to as dimensionless separation factor (R_L), defined as (Sadaf et al., 2015):

$$R_L = \frac{1}{1 + K_L C_o} \tag{5}$$

with C_o standing for the highest 4CG initial concentration. Unfavorable adsorption is described by $R_L > 1$, linear if $R_L = 1$, favorable for 0, $(0 < R_L < 1)$ as well as irreversible adsorption if $R_L = 0$.

Second most widely used isotherm model is Freundlich isotherm postulated base on surfaces that are heterogeneous. Its logarithmic form is expressed as (Freundlich, 1906):

$$\log q_e = \log K_F + \frac{1}{n} \log C_e \tag{6}$$

with the two constants symbolized as K_F and n measuring the adsorption capacity of the adsorbent as well as how the model

Table 1 Linear forms of Langmuir isotherm.

Isotherm	Linear form	Plot
Langmuir-1	$\frac{1}{q_e} = \frac{1}{K_L Q_a^o C_e} + \frac{1}{Q_a^o}$	$\frac{1}{q_e}$ vs $\frac{1}{C_e}$
Langmuir-2	$\frac{C_e}{q_e} = \frac{C_e}{Q_a^o} + \frac{1}{K_L Q_a^o}$	$\frac{C_e}{q_e}$ vs C_e
Langmuir-3	$q_e = -\frac{q_e}{K_L C_e} + Q_a^o$	q_e vs $\frac{q_e}{C_e}$
Langmuir-4	$\frac{q_e}{C_e} = -K_L q_e + K_L Q_a^o$	$\frac{q_e}{C_e}$ vs q_e
Langmuir-5	$\frac{1}{C_e} = \frac{K_L Q_a^o}{q_e} - K_L$	$\frac{1}{C_e}$ vs $\frac{1}{q_e}$

deviates from linearity, respectively. Generally, $n > 1$ suggests favorable adsorption of adsorbate on the adsorbent. The greater the value of n, the more sturdy the adsorption strength.

Temkin model was based on how indirect adsorbent/adsorbate interactions influence the adsorption isotherms. Its linear form is expressed as (Temkin and Pyzhev, 1940):

$$q_e = \frac{RT}{b}\ln A + \frac{RT}{b}\ln C_e \quad (7)$$

where $\frac{R_T}{b} = B$ (J/mol) and A (L/g) are Temkin constants, which are related to heat of sorption and maximum binding energy, respectively, R is the gas constant (8.31 J/mol K) and T (K) is the absolute temperature.

To compare the validity of each model, chi square (χ^2) was incorporated since correlation coefficient (R^2) may not justify the basis for selecting the best adsorption model because it only signifies the fit between linear forms of the isotherm equations and experimental data and while the suitability between experimental and predicted values of the adsorption capacity is described by chi square (χ^2). The lower the χ^2 value, the better the fit.

Table 2 summarizes the parameters obtained from the adsorption isotherm models applied with their respective R^2 and χ^2 values. The Langmuir parameters obtained from the five linear equations were not the same as can be observed from Table 2, because the transformations change the original error distribution (Baccar et al., 2013). Based on the R^2 values, the best fit should have been Langmuir-1 or Langmuir-5 isotherms in comparison with the other isotherm equations because they showed the largest values ($R^2 = 0.9986$).

But according to Baccar et al. (2013) the highest R^2 does not necessarily describe the most superlative transformation. So as observed from Table 2, Langmuir-1 and 5 had the highest R^2 values ($R^2 = 0.9986$) but their χ^2 values (1.130) were also larger, higher than Langmuir-2 (0.234), therefore they cannot be concluded to perfectly describe the equilibrium data. It can also be seen from Table 2 that χ^2 value of the Langmuir-2 isotherm (0.234) was lower than those obtained from the Freundlich (0.759) and Temkin (59.859), therefore, the maximum adsorption capacity (Q_a^0), sorption energy (K_L) and separation factor (R_L) values of 498.67 mg/g, 0.038 and 0.069, respectively were adopted from the Langmuir-2 equation.

The high Q_a^0 of 498.67 mg/g observed in this study was attributed to the relatively high surface area of the PASH-AC and its mesoporous structure (Garba and Afidah, 2014). It compares well with those obtained from the literature as summarized in Table 3.

Table 2 Langmuir (1–5), Freundlich and Temkin isotherm model parameter correlation coefficients and chi square values for 4CG adsorption on PASH-AC at 30 °C.

Isotherm	Parameters			
	Q_a^0 (mg/g)	R_L	R^2	χ^2
Langmuir				
Langmuir-1	407.29	0.054	0.9986	1.130
Langmuir-2	498.67	0.069	0.9957	0.234
Langmuir-3	481.57	0.067	0.9792	8.728
Langmuir-4	493.09	0.055	0.9792	1.420
Langmuir-5	413.59	0.055	0.9986	2.860
	K_F (mg/g (L/mg)	n	R^2	χ^2
Freundlich	2.3276	1.382	0.9904	0.759
	A (L/g)	B (J/mol)	R^2	χ^2
Temkin	0.644	85.518	0.9470	59.859

3.5. Adsorption kinetic studies

The kinetics of 4CG adsorption was investigated by applying Lagergren pseudo-first order and pseudo-second order (1 and 2) models. The pseudo-first-order linear equation was given as (Lagergren and Svenska, 1898):

$$\log(q_e - q_t) = \log q_e - \frac{k_1}{2.303}t \quad (8)$$

where k_1 is the pseudo-first-order rate constant (h^{-1}).

The two linear forms of pseudo-second-order equations were expressed as Eqs. (9) and (10):

$$\frac{t}{q_t} = \frac{1}{k_2 q_e^2} + \frac{1}{q_e}t \quad (9)$$

$$\frac{1}{q_t} = \left(\frac{1}{k_2 q_e^2}\right)\frac{1}{t} + \frac{1}{q_e} \quad (10)$$

where k_2 (g/mgh) is the pseudo-second-order rate constant.

The values of q_e, k_1, R^2 and χ^2 obtained after the linear plots of Eq. (8) and q_e, k_2, R^2 and χ^2 from the plots of Eqs.

Table 3 Comparison of maximum monolayer adsorption capacity of various CPs on different adsorbents.

Adsorbent	Adsorbate	Q_a^0 (mg/g)	References
PASH-AC	4-Chloroguaiacol	498.67	This work
Commercial activated carbon	4-Chloroguaiacol	276.88	This study
Oil palm shell activated carbon	4-Chloroguaiacol	454.45	Hamad et al. (2010)
Oil palm shell activated carbon	4-chloro2-methoxy phenol	323.62	Hamad et al. (2011)
Rattan sawdust based activated carbon	4-chlorophenol	188.68	Hameed et al. (2008)
Cattail fibre-based activated carbon	2,4-Dichlorophenol	142.86	Ren et al. (2011)
Rice straw carbon	3-chlorophenol	14.2	Wang et al. (2007)

Table 4 Pseudo-first-order and pseudo-second-order (1 and 2) kinetic model parameters of 4CG adsorption on PASH-AC at 30 °C.

C_o (mg/L)	$q_{e,exp}$ (mg/g)	Pseudo-first-order				Pseudo-second-order-1				Pseudo-second-order-2			
		k_1 (1/h)	$q_{e,cal}$ (mg/g)	R^2	χ^2	k_2 (g/mg h)	$q_{e,cal}$ (mg/g)	R^2	χ^2	k_2 (g/mg h)	$q_{e,cal}$ (mg/g)	R^2	χ^2
30	28.51	0.330	14.73	0.981	0.234	0.100	26.88	0.996	0.003	0.178	24.57	0.960	0.019
60	56.60	0.482	41.21	0.989	0.074	0.023	59.52	0.997	0.003	0.029	55.87	0.998	0.001
100	93.81	0.377	57.73	0.988	0.148	0.021	90.91	0.992	0.001	0.037	81.97	0.969	0.016
150	139.31	0.430	89.78	0.997	0.126	0.013	138.89	0.993	0.009	0.026	120.48	0.958	0.018
250	228.38	0.356	134.15	0.978	0.170	0.010	217.39	0.995	0.002	0.016	200.00	0.972	0.015
350	307.86	0.421	215.48	0.990	0.090	0.005	312.50	0.996	0.002	0.0064	285.71	0.991	0.005

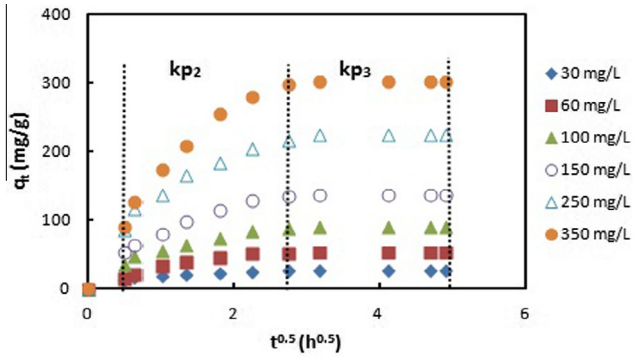

Figure 4 Plot of intraparticle diffusion model for adsorption of 4CG onto PASH-AC at 30 °C.

(9) and (10) (figures not shown) for the 4CG adsorption on the PASH-AC are reported in Table 4.

As can be observed from Table 4, the trends of R^2 values (0.981–0.997) for the pseudo-first-order model were not coherent. Also, the calculated and experimental q_e values were not in good concord with each other, indicating the inappropriateness of pseudo first-order kinetic model in describing 4CG adsorption onto PASH-AC. However, the harmony between experimental and calculated q_e values obtained from pseudo-second-order (1 and 2) models were lofty with all the R^2 values obtained very near to unity, confirming that the most suitable model to describe 4CG adsorption onto PASH-AC was pseudo-second-order model. To further confirm the suitability of these kinetic models in describing the 4CG adsorption process, chi-square (χ^2) statistical analysis was also applied. As can be observed from Table 4, the χ^2 values acquired from both the pseudo-second-order 1 and 2 models (0.001–0.019) were lower than those obtained from the pseudo-first-order (0.074–0.234) which further confirms the pseudo-second-order equation to be the most preeminent kinetic model in describing the 4CG adsorption onto PASH-AC.

The kinetic models were limited in terms of identifying the diffusion mechanisms as well as the rate controlling steps in the adsorption process, as result of that limitation; intraparticle diffusion model was further applied. The intraparticle diffusion equation is expressed as:

$$q_t = k_{ip} t^{1/2} + C \tag{11}$$

where k_{ip} is rate constant of the intra-particle diffusion equation and C gives information about the boundary layer thickness: larger value of C is associated with the boundary layer diffusion effect. When the linear plot q_t versus $t^{1/2}$ is linear and passes through the origin, it connotes that the adsorption process follows the intraparticle diffusion model, and that the only rate limiting step involved is intraparticle diffusion, if not, then it connotes that intraparticle diffusion is not the only rate limiting step involved (Fan et al., 2011).

The intraparticle diffusion plots for the adsorption of 4CG on PASH-AC at 30 °C are depicted by Fig. 4.

As can be seen from Fig. 4, a very rapid adsorption was described by the first sharper region completed attributed to a strong electrostatic attraction between 4CG and the PASH-AC external surface. The next stage describes a steady adsorption stage, which can be attributed to intraparticle

Table 5 Intraparticle diffusion model parameters for the adsorption of 4CG onto PASH-AC.

C_o (mg/L)	Intraparticle diffusion model					
	k_{p2} (mg/g h$^{1/2}$)	k_{p3} (mg/g h$^{1/2}$)	C_2	C_3	$(R_2)^2$	$(R_3)^2$
30	6.847	–	11.007	25.750	0.9561	–
60	20.593	0.2227	9.692	52.633	0.9534	0.4919
100	26.770	0.5229	27.354	87.648	0.9660	0.4919
150	42.560	0.2742	37.794	135.630	0.9835	0.4919
250	64.115	–	69.124	–	0.9498	–
350	106.980	–	55.924	–	0.9639	–

Table 6 Thermodynamic parameters for the adsorption of 4CG onto PASH-AC at different temperatures.

ΔH (kJ/mol)	ΔS (J/mol K)	ΔG (kJ/mol)		
		303 K	313 K	323 K
1.49	24.30	−5.94	−5.96	−6.43

diffusion of the 4CG molecule through the activated carbon's pores. Third stage exists in few cases, especially when the 4CG initial concentrations are high. At that stage, the intraparticle diffusion starts to slow down (Wang et al., 2010).

The values of k_{pi}, C_i and R^2 obtained are given in Table 5. The values of k_{p2} as can be seen from Table 5 increased with upsurge in the initial 4CG concentration, which was attributed to the greater driving force. The values of C_2 and C_3 also increased with the increase in 4CG concentration from 30 to 350 mg/L signifying an increase in the thickness of the boundary layer (Khaled et al., 2009).

In the second and third stages as can be observed from Fig. 4, the linear lines did not pass through the origin which suggested the presence of intraparticle diffusion along with possibility of involvement of some other rate controlling steps in the adsorption process (Maksin et al., 2012).

3.6. Adsorption thermodynamic studies

Gibb's free energy change (ΔG), enthalpy change (ΔH) and entropy change (ΔS) are the most popular thermodynamic parameters that were considered and studied in this work. Van't Hoff equation was employed in determining the thermodynamic parameters which was expressed as (Slimani et al., 2014):

$$\ln K_D = \frac{\Delta S}{R} - \frac{\Delta H}{RT} \tag{12}$$

where R (8.314 kJ/mol) is the universal gas constant; T (K) is the absolute temperature; $K_D = \frac{q_e}{C_e}$ is the distribution coefficient; q_e (mg/g) is the amount of adsorbate adsorbed on the sorbent per unit mass. A linear plot of $\ln K_D$ against $1/T$ gives a graph (Fig. not shown) with ΔH and ΔS obtained from the slope and intercept respectively. ΔG was evaluated from the relation below:

$$\Delta G = -RT \ln K_D \tag{13}$$

The thermodynamic parameters obtained for the adsorption of the 4CG on PASH-AC at three different temperatures are reported in Table 6.

Positive values were obtained for both ΔH and ΔS, implying that the 4CG adsorption process was endothermic with random characteristics. The Gibb's free energy of change was spontaneous as can be seen by the negative values obtained. The ΔG values also confirmed the adsorption of 4CG onto PASH-AC to be a physical process with the physical adsorption values ranging from −20 to 0 kJ/mol while value from −80 to −400 kJ/mol describes chemical adsorption (Li et al., 2010).

4. Conclusions

PASH-AC was produced from *Prosopis africana* seed hulls. Its adsorption capacity was observed to be increasing with an upsurge in both adsorption time as well as initial 4CG concentration. The adsorption process was more promising in lower pH solution with the Langmuir-2 model being the most appropriate in describing the equilibrium data. The kinetics data obeyed pseudo-second-order model. 4CG adsorption onto PASH-AC was primarily presided by particle diffusion according to the Boyd plot. The positive ΔH values observed connoted the adsorption process to be endothermic. The adsorption potential of the PASH-AC competed satisfactorily with earlier studied adsorbents. Based on the obtained results, the PASH-AC produced can be used effectively to tackle pollution problems posed by chloroguaicols in the environment.

Acknowledgement

Research University Grant 1001/PKIMIA/854002 from Universiti Sains Malaysia that ensued in this article was recognized by the authors.

References

Baccar, R., Blánquez, P., Bouzid, J., Feki, M., Attiya, H., Sarrà, M., 2013. Modeling of adsorption isotherms and kinetics of a tannery dye onto an activated carbon prepared from an agricultural by-product. Fuel Process. Technol. 106, 408–415.

El Haddad, M., Mamouni, R., Saffaj, N., Lazar, S., 2012. Removal of a cationic dye – Basic Red 12 – from aqueous solution by adsorption onto animal bone meal. J. Assoc. Arab Univ. Basic Appl. Sci. 12, 48–54.

El Haddad, M., Slimani, R., Mamouni, R., ElAntri, S., Lazar, S., 2013. Removal of two textile dyes from aqueous solutions onto calcined bones. J. Assoc. Arab Univ. Basic Appl. Sci. 14, 51–59.

Fan, J., Zhang, J., Zhang, C., Ren, L., Shi, Q., 2011. Adsorption of 2,4,6-trichlorophenol from aqueous solution onto activated carbon derived from loosestrife. Desalination 267, 139–146.

Freundlich, H.M.F., 1906. Over the adsorption in solution. J. Phys. Chem. 57, 385–470.

Galadima, A., Garba, Z.N., Leke, L., Almustapha, M.N., Adam, I.K., 2011. Domestic water pollution among local communities in nigeria—causes and consequences. Eur. J. Sci. Res. 52 (4).

Garba, Z.N., Afidah, A.R., 2014. Process optimization of $K_2C_2O_4$-activated carbon from *Prosopis africana* seed hulls using response surface methodology. J. Anal. Appl. Pyrol. 107, 306–312.

Garba, Z.N., Afidah, A.R., Hamza, S.A., 2014. Potential of borassus aethiopum shells as precursor for activated carbon preparation by physico-chemical activation; optimization, equilibrium and kinetic studies. J. Environ. Chem. Eng. 2, 1423–1433.

Hamad, B.K., Noor, A.M., Afida, A.R., Mohd Asri, M.N., 2010. High removal of 4-chloroguaiacol by high surface area of oil palm shell-activated carbon activated with NaOH from aqueous solution. Desalination 257 (1–3), 1–7.

Hamad, B.K., Ahmad, M.N., Afidah, A.R., 2011. Removal of 4-chloro-2-methoxy phenol by adsorption from aqueous solution using oil palm shell carbon activated by K_2CO_3. J. Phys. Sci. 22, 41–58.

Hameed, B.H., Chin, L.H., Rengaraj, S., 2008. Adsorption of 4-chlorophenol onto activated carbon prepared from rattan sawdust. Desalination 225 (1–3), 185–198.

Jodeh, S., Abdelwahab, F., Jaradat, N., Warad, I., Jodeh, W., 2016. Adsorption of diclofenac from aqueous solution using *Cyclamen persicum* tubers based activated carbon (CTAC). J. Assoc. Arab Univ. Basic Appl. Sci. 20, 32–38.

Khaled, A., El-Nemr, A., El-Sikaily, A., Abdelwahab, O., 2009. Removal of Direct N Blue106 from artificial textile dye effluent

using activated carbon from orange peel: adsorption isotherm and kinetic studies. J. Hazard. Mater. 165, 100–110.

Lagergren, S., Svenska, B.K., 1898. On the theory of so-called adsorption of dissolved substances. R. Swed. Acad. Sci. Doc. 24, 1–13.

Langmuir, I., 1916. The constitution and fundamental properties of solids and liquids part I solids. J Am. Chem. Soc. 38, 2221–2295.

Li, Q., Yue, Q., Su, Y., Gao, B., Sun, H., 2010. Equilibrium, thermodynamics and process design to minimize adsorbent amount for the adsorption of acid dyes onto cationic polymer-loaded bentonite. Chem. Eng. J. 158, 489–497.

Maksin, D.D., Nastasović, A.B., Milutinović-Nikolić, A.D., Suručić, L.T., Sandić, Z.P., Hercigonja, R.V., Onjia, A.E., 2012. Equilibrium and kinetics study on hexavalent chromium adsorption onto diethylene triamine grafted glycidyl methacrylate based copolymers. J. Hazard. Mater. 209, 99–110.

Noreen, S., Bhatti, H.N., 2014. Fitting of equilibrium and kinetic data for the removal of Novacron Orange P-2R by sugarcane bagasse. J. Ind. Eng. Chem. 20, 1684–1692.

Noreen, S., Bhatti, H.N., Nausheen, S., Sadaf, S., Ashfaq, M., 2013. Batch and fixed bed adsorption study for the removal of Drimarine Black CL-B dye from aqueous solution using a lignocellulosic waste: a cost affective adsorbent. Ind. Crops Prod. 50, 568–579.

Ren, L., Zhang, J., Li, Y., Zhang, C., 2011. Preparation and evaluation of cattail fiber-based activated carbon for 2,4-dichlorophenol and 2,4,6-trichlorophenol removal. Chem. Eng. J. 168, 553–561.

Sadaf, S., Bhatti, H.N., Nausheen, S., Amin, M., 2015. Removal of Cr (VI) from wastewater using acid-washed zero-valent iron catalyzed by polyoxometalate under acid conditions: efficacy, reaction mechanism and influencing factors. J. Taiwan Inst. Chem. Eng. 47, 160–170.

Shi, Q.Q., Zhang, J., Zhang, C.L., Li, C., Zhang, B., Hu, W.W., Xu, J. T., 2010. Preparation of activated carbon from cattail and its application for dyes removal. J. Environ. Sci. 22, 91–97.

Slimani, R., El Ouahabi, I., Abidi, F., El Haddad, M., Regti, A., Laamari, M., El Antri, S., Lazar, S., 2014. Calcined eggshells as a new biosorbent to remove basic dye from aqueous solutions: thermodynamics, kinetics, isotherms and error analysis. J. Taiwan Inst. Chem. Eng. 45, 1578–1587.

Temkin, M.J., Pyzhev, V., 1940. Recent modifications to Langmuir isotherms. Acta Physicochim. 12, 217–222.

Wang, S.L., Tzou, Y.M., Lu, Y.H., Sheng, G., 2007. Removal of 3-chlorophenol from water using rice-straw-based carbon. J. Hazard. Mater. 147, 313–318.

Wang, L., Zhang, J., Zhao, R., Li, C., Li, Y., Zhang, C., 2010. Adsorption of basic dyes on activated carbon prepared from Polygonum orientale Linn: equilibrium, kinetic and thermodynamic studies. Desalination 254, 68–74.